G.G. Adamian

SHE – Production Mechanisms

Discussion Contribution

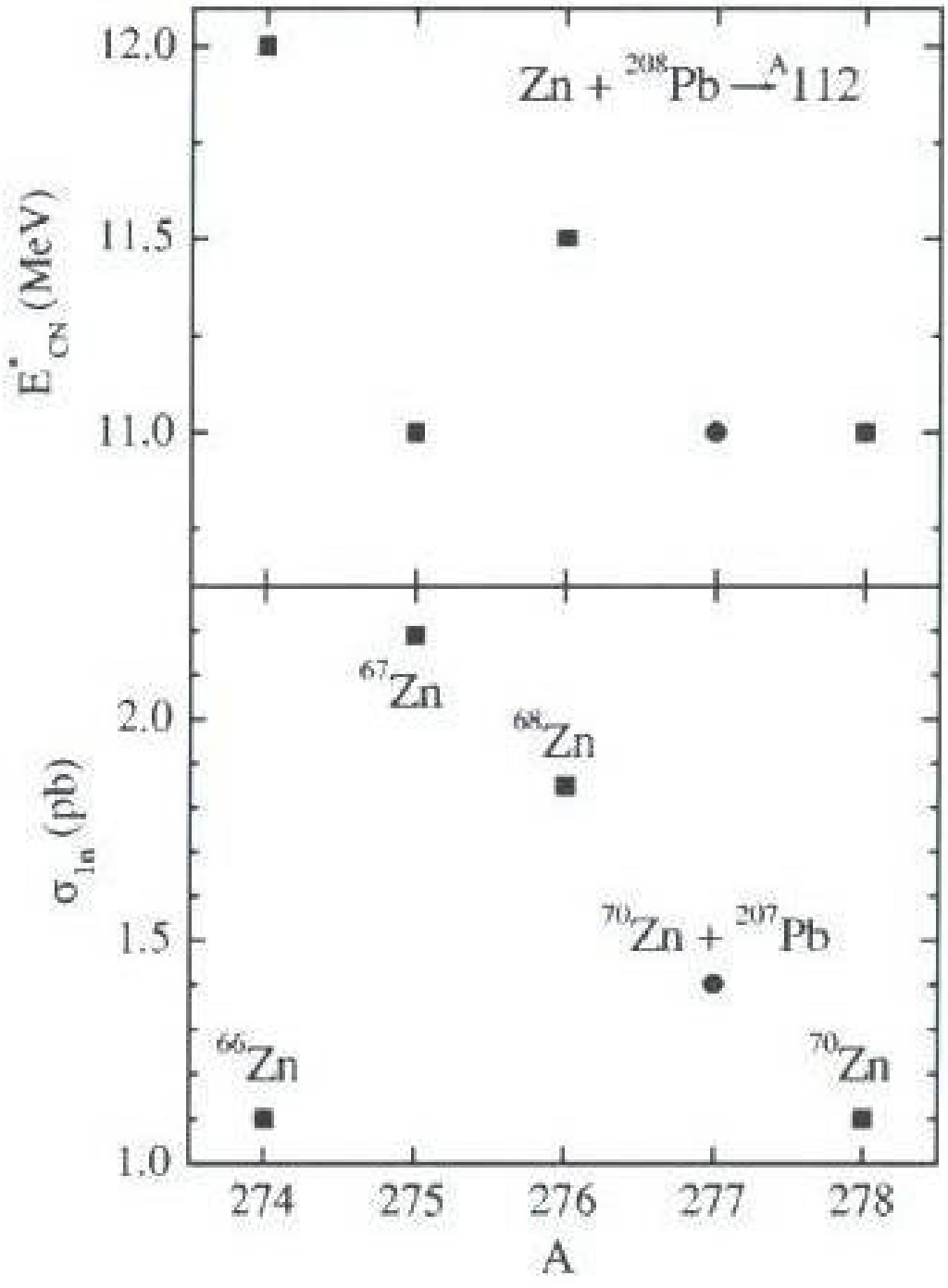

FIG. 3. The same as in Fig. 2, but for the fusion reactions Zn $+{}^{208}Pb \rightarrow {}^{A}112$ and ${}^{68}Zn + {}^{207}Pb \rightarrow {}^{275}112$.

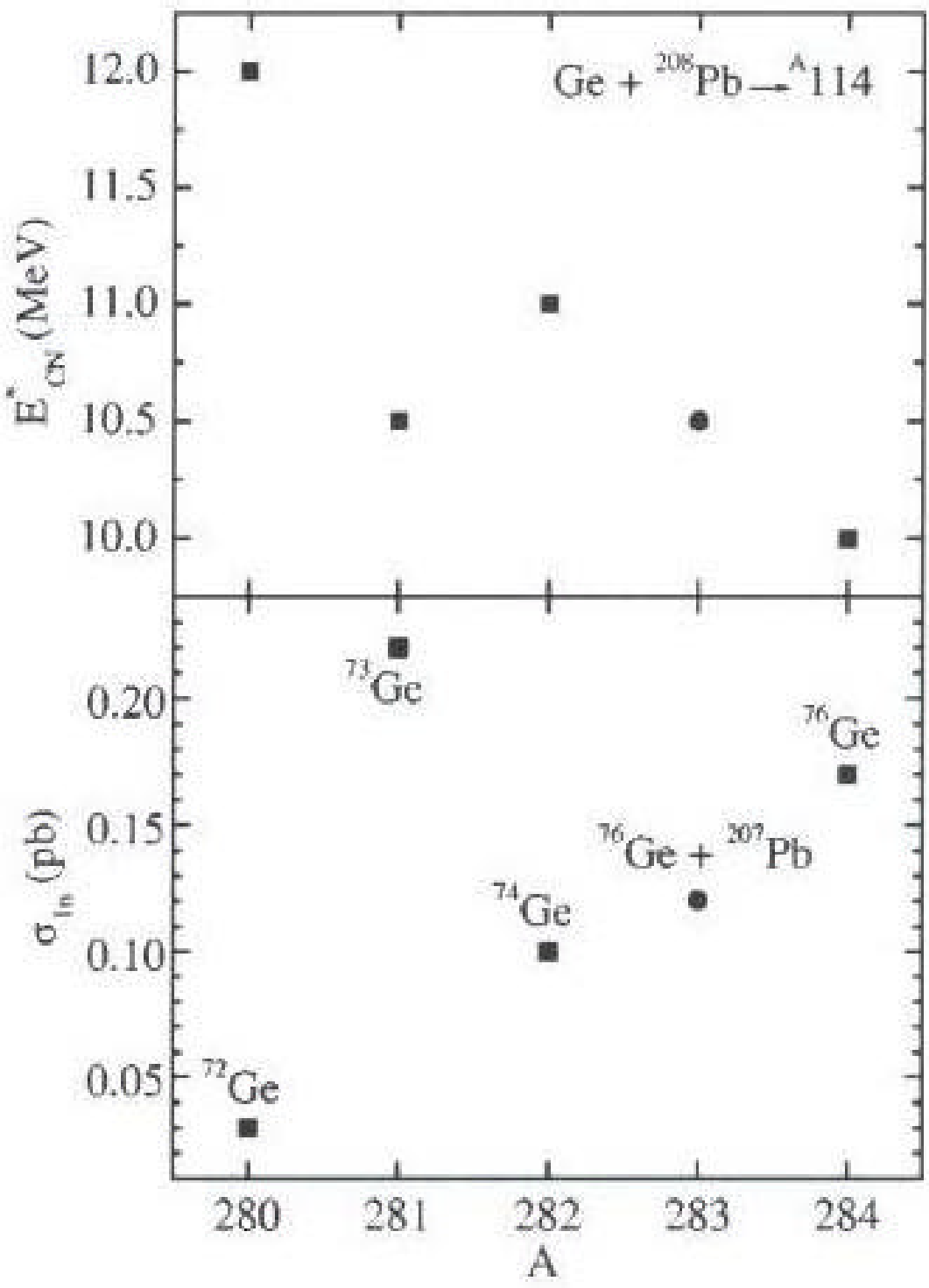

FIG. 4. The same as in Fig. 2, but for the fusion reactions Ge + ^{208}Pb → ^{A}114 and ^{76}Ge + ^{207}Pb → ^{283}114.

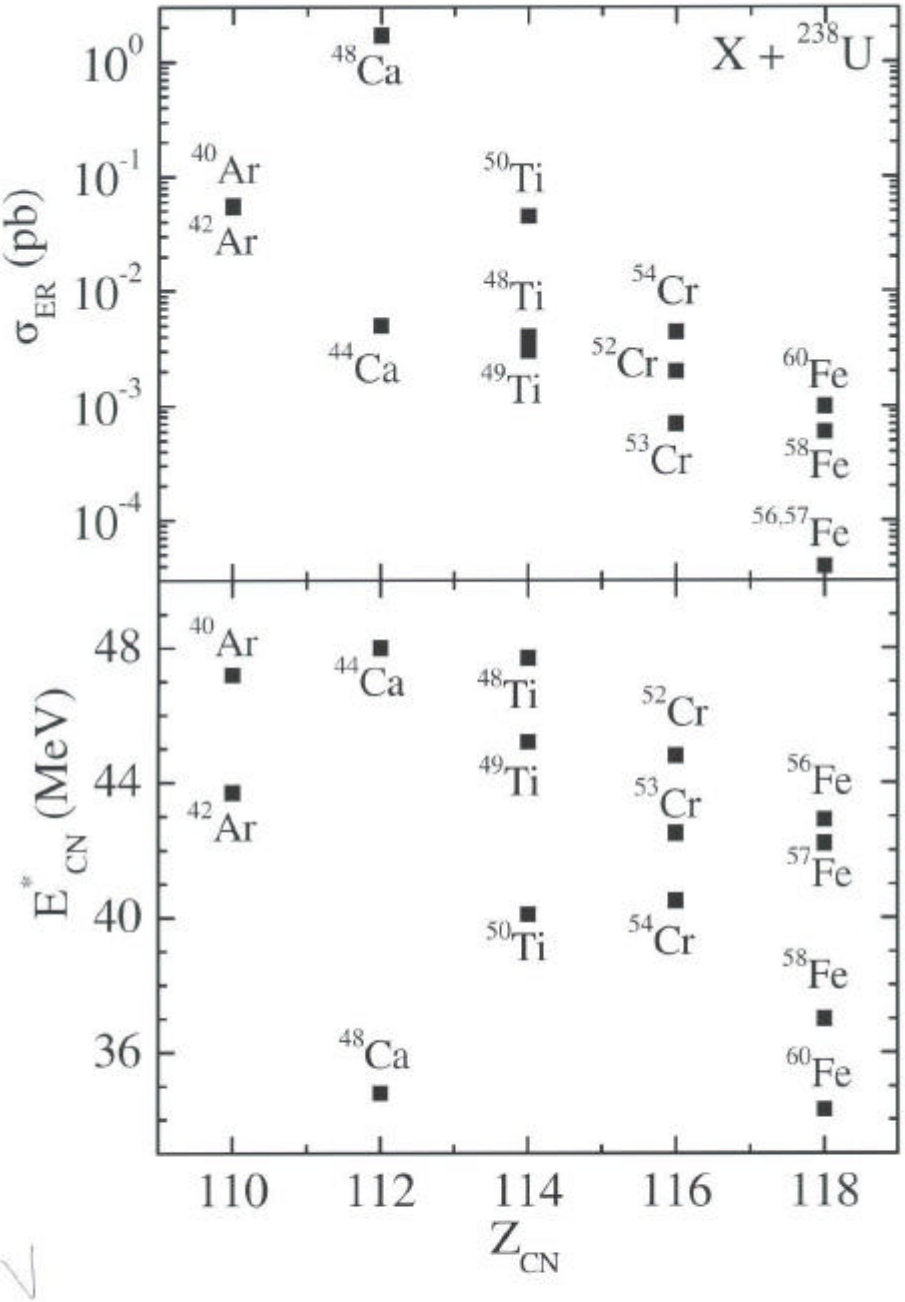
X + 238U
σER (pb)
10^0
10^-1
10^-2
10^-3
10^-4
48Ca
40Ar
42Ar
50Ti
48Ti
49Ti
44Ca
54Cr
52Cr
53Cr
60Fe
58Fe
56,57Fe
E*CN (MeV)
48
44
40
36
40Ar
42Ar
44Ca
48Ca
48Ti
49Ti
50Ti
52Cr
53Cr
54Cr
56Fe
57Fe
58Fe
60Fe
110
112
114
116
118
ZCN

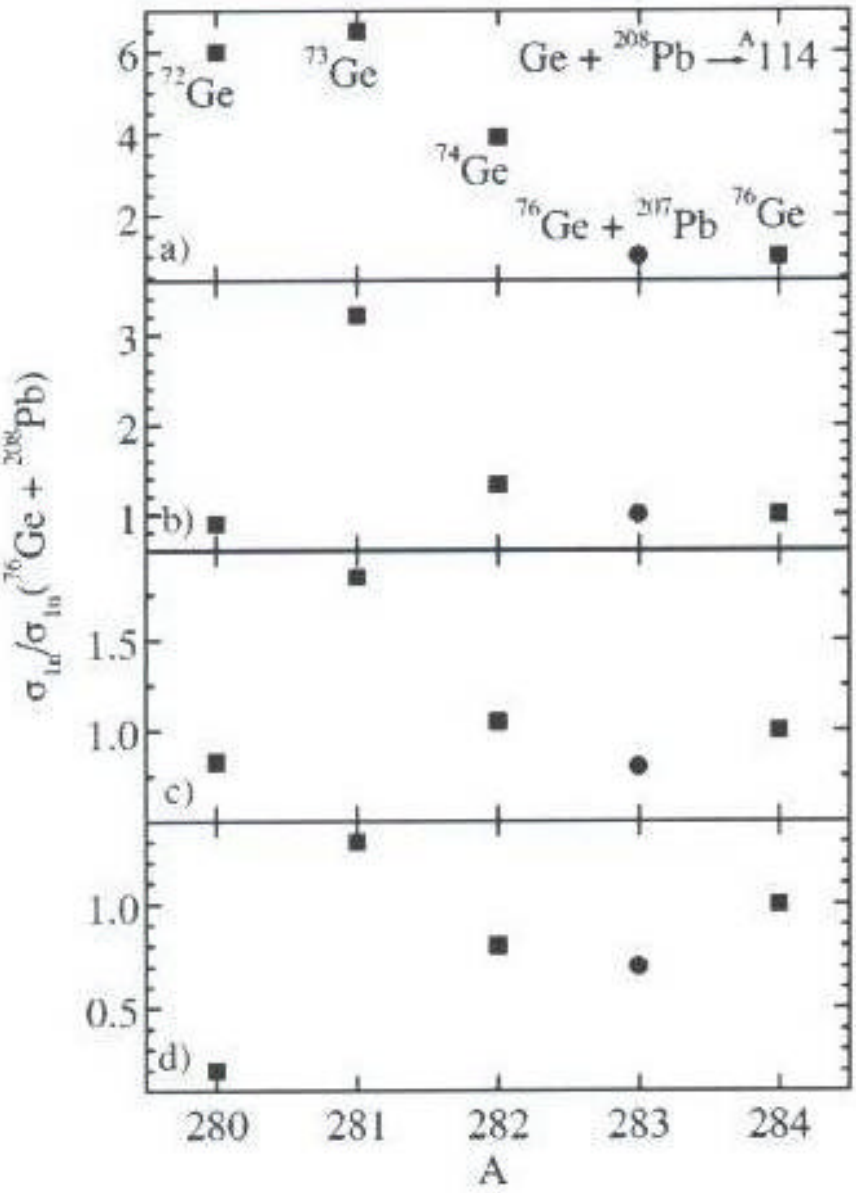

FIG. 5. The calculated ratios between the maximal production cross sections in the reactions Ge+Pb$\rightarrow{}^{A}$114 and ^{76}Ge+^{208}Pb $\rightarrow{}^{284}$114 as functions of A. The results obtained with data of Ref. [21], of finite range droplet model [20], of finite range liquid drop model [20], and of Ref. [17] are shown from upper part to lower part, respectively.

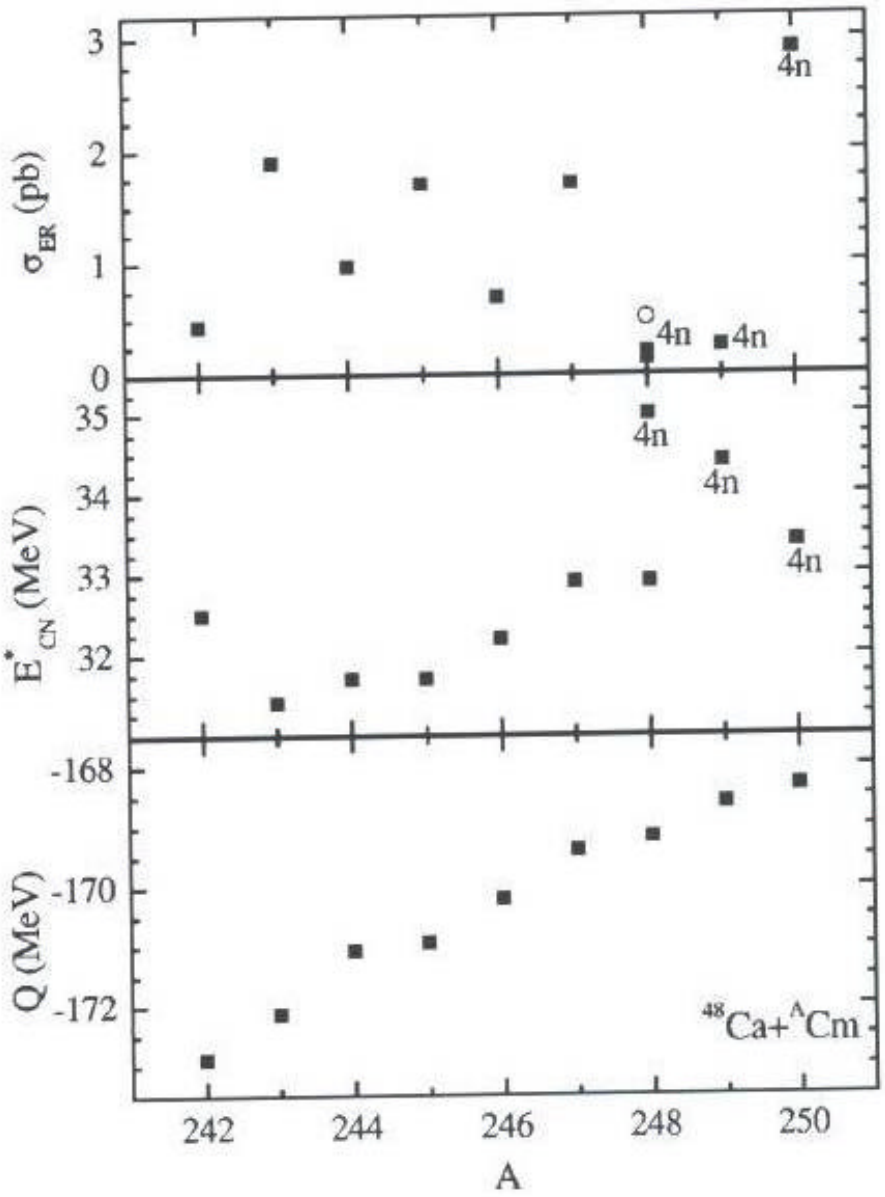

FIG. 4. The same as in Fig. 1, but for the fusion reactions ^{48}Ca+^{A}Cm. The maximal evaporation residue cross sections in the $4n$ channel (upper part) at the corresponding excitation energies of compound nuclei (middle part) are indicated. The experimental data of the reactions $^{48}\mathrm{Ca}+^{248}\mathrm{Cm}\rightarrow{}^{292}116+4n$ ($E^*_{CN}\approx 31-36$ MeV) [3] are presented by an open circle.